Cellular Applications of ^{31}P and ^{13}C Nuclear Magnetic Resonance

R. G. Shulman, T. R. Brown, K. Ugurbil, S. Ogawa
S. M. Cohen, J. A. den Hollander

Summary. High-resolution nuclear magnetic resonance (NMR) studies of cells and purified mitochondria are discussed to show the kind of information that can be obtained in vivo. In suspensions of *Escherichia coli* both phosphorus-31 and carbon-13 NMR studies of glycolysis and bioenergetics are presented. In rat liver cells the pathways of gluconeogenesis from carbon-13–labeled glycerol are followed by carbon-13 NMR. In the intact liver cells cytosolic and mitochondrial *p*H's were separately measured by phosphorus-31 NMR. In purified mitochondria the internal and external concentrations of inorganic phosphate, adenosine diphosphate, and adenosine triphosphate were determined by phosphorus-31 NMR while the *p*H difference across the membrane was measured simultaneously.

Nuclear magnetic resonance (NMR) spectroscopy has been extensively used in the field of biochemistry, primarily in studies of biological macromolecules. Recently, NMR studies have been extended to intact cells, organelles, and organs. Consequently, it is now possible to obtain on metabolites in vivo the kinds of detailed information about structure, motion, reaction rates, and binding sites that have been obtained by NMR studies of purified biomolecules in solution. Numerous investigations of intact systems by means of phosphorus-31 NMR have already been reported. These include studies of red blood cells (*1-3*), yeast (*4*), Erhlich ascites tumor cells (*5*), muscle (*6, 7*), perfused rat hearts (*8, 9*), kidneys (*10*), cultured mammalian cells (*11, 12*), blood platelets (*13, 14*), and chromaffin granules (*15*). The early work has previously been reviewed (*16*). In this article we survey some of our recent ^{31}P and ^{13}C NMR studies of suspensions of *Escherichia coli* (*17-21*), rat liver cells (*22-24*), and purified rat liver mitochondria (*25*), and describe the kinds of information available from this approach. By using ^{31}P NMR we have measured intracellular *p*H and the concentrations and distribution of phosphorylated metabolites such as adenosine triphosphate (ATP), adenosine diphosphate (ADP), and inorganic phosphate (P_i), and here we demonstrate how the changes in *p*H and the time development of these compounds can be followed simultaneously. We also show how saturation transfer measurements on ATP and P_i can be used to follow specific enzymatic rates in vivo.

Although ^{13}C NMR has been used in the past to follow the end products of metabolic pathways (*26, 27*) and the reaction products in acetone-treated cells (*28*), only recently have we used this approach to follow metabolic intermediates in cells (*21, 23, 24*). The ^{13}C NMR experiments on *E. coli* and liver cells discussed here, where ^{13}C-enriched substrates have been metabolized by the cells, show how resonances from both the intermediates and end products of metabolism can be observed and the distribution of the label used to elucidate pathways and kinetics. The ^{13}C and ^{31}P nuclei in many ways yield complementary data and, when used on the same system, supply a tremendous amount of simultaneous information about metabolic functioning in vivo.

Phosphorus-31 NMR

Before discussing the ^{31}P NMR experiments we will review briefly the present understanding of oxidative phosphorylation and transport. These ideas were originally suggested by Mitchell (*29*) and have been supported by many experiments (*30*), including our own.

Figure 1 shows the two pathways involved in energetics according to the chemiosmotic hypothesis. Using the energy of electron transfer from a suitable electron donor to O_2, mitochondria and some bacteria can generate a transmembrane *p*H gradient (ΔpH) and an electrical potential ($\Delta\psi$) by translocation of protons. This proton electrochemical potential gradient is subsequently utilized for many purposes, in particular for transport of substances across the membranes and for ATP synthesis by the reversible membrane-bound enzyme, adenosinetriphosphatase (ATPase) (*31*). In the case of facultative aerobes, such as *E. coli*, ATP can also be produced in the absence of oxygen by substrate level phosphorylation of ADP during fermentation of a carbon source such as glucose. The ATPase then functions in reverse, creating a proton electrochemical potential gradient by hydrolyzing the ATP.

Escherichia coli

These ideas can be investigated by using ^{31}P NMR because concentrations of ATP, ADP, and P_i can be measured simultaneously with ΔpH. This is illustrated in Fig. 2, which presents the intact cell ^{31}P NMR spectrum under anaerobic conditions of freshly harvested *E. coli* cells, before and approximately 5 minutes after the addition of glucose (*20*). These and the other spectra discussed in this article were measured by means of a Bruker HX-360 spectrometer operating in the Fourier transform mode. The resonances were assigned to specific metabolites on the basis of chemical shifts, their dependence on *p*H in extracts and, when necessary, were confirmed by adding the assigned compound to the extracts. The specific assignments are given in the figure.

Several interesting changes occur in the spectrum after glucose addition. Before glucose addition the 5- to 19-part-per-million (ppm) region of the spectrum is dominated by nucleoside diphosphate (NDP) peaks; after glucose addition the spectrum is dominated by nucleoside triphosphate (NTP) peaks.

The other significant difference between A and B in Fig. 2 is the low field region (−3 to −5 ppm) which typically contains resonances from phospho-

The authors are all at the Bell Laboratories, Murray Hill, New Jersey 07974, where R. G. Shulman is head of biophysics research, T. R. Brown and S. Ogawa are members of the technical staff, K. Ugurbil is a postdoctoral fellow, and S. M. Cohen and J. A. den Hollander are postdoctoral consultants. In addition, S. M. Cohen is a research associate of Princeton University and J. A. den Hollander is a consultant at Brookhaven National Laboratories.

0036-8075/79/0713-0160$01.75/0

monoesters such as sugar phosphates. Before glucose addition the broad phosphomonoester resonance in this region includes contributions from several compounds that have been assigned to glycolytic intermediates and nucleoside monophosphates (*18*). Afterward, however, it is dominated by the intense peak from the β anomer of fructose 1,6-bisphosphate (FBP) (Fig. 2B). This compound is present in large amounts only during glycolysis and is the major intermediate during this process.

The critical role assigned to the membrane-bound enzyme ATPase by the chemiosmotic model has been examined by ^{31}P NMR with the use of ATPase inhibitors, uncouplers, and mutant strains (ATPase$^-$) that are deficient in ATPase activity. If the ΔpH observed after glucose addition (Fig. 2B) is created by the ATPase hydrolyzing ATP and simultaneously extruding protons out of the cell, then the magnitude of the ΔpH generated should be reduced in cells treated with dicyclohexylcarbodiimide (DCCD), an inhibitor of the ATPase, or in *E. coli* ATPase$^-$ mutants. In both DCCD-treated and ATPase$^-$ cells NMR experiments showed a ΔpH of <0.1 (indicated by an unsplit P_i peak), and higher NTP to NDP ratios during glucose catabolism under anaerobic conditions. In addition, with the ATPase pathway blocked, the NTP lasted several times longer after glucose was exhausted. This indicates that the major pathway of ATP use under our experimental conditions was through ATPase, where it was hydrolyzed to create a ΔpH across the cell membrane. Both the DCCD-treated and ATPase$^-$ cells were shown by ^{31}P NMR to have intact and functioning electron transport chains capable of generating a ΔpH in the presence of lactate and O_2.

In other experiments, *E. coli* cells were allowed to catabolize glucose in the presence of the uncoupler *p*-trifluoromethoxyphenylhydrazone (FCCP) that transports protons across the cellular membrane, thereby destroying *p*H gradients. Under these conditions, once again, a single P_i peak was observed, showing that $\Delta pH = 0$. However, unlike the DCCD-inhibited cells, there was little sign of NTP even though glucose was being utilized. This presumably occurred because NTP was consumed much faster than usual as the cells rapidly hydrolyzed it in an attempt to create a proton gradient. In agreement with this, prior treatment with DCCD to inhibit the ATPase counteracted the FCCP effect on the NTP levels; while these cells did not produce a ΔpH, they accumulated high concentrations of NTP.

Mitochondria

In eukaryotic cells, the site of oxidative phosphorylation is the mitochondria. The mitochondrial electron transport chain creates a proton electrochemical potential gradient across the mitochondrial membrane. The energy contained in this gradient is subsequently used to synthesize ATP by the mitochondrial ATPase. Figure 3 illustrates the ^{31}P NMR spectra obtained from a suspension of purified rat liver mitochondria under anaerobic and aero-

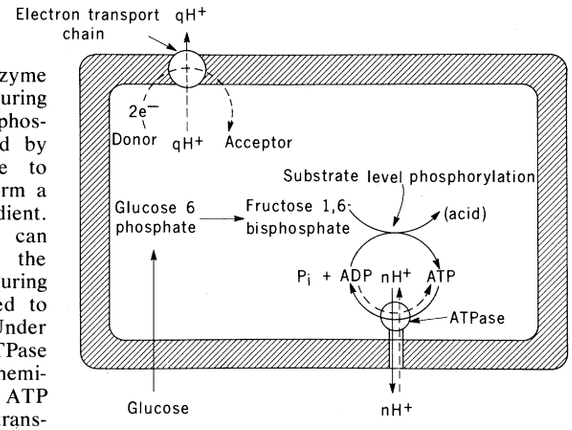

Fig. 1. Schematic view of an *E. coli* cell, demonstrating the linkage between substrate level phosphorylation, oxidative phosphorylation, and the enzyme ATPase. The ATP formed during glycolysis by substrate level phosphorylation can be hydrolyzed by the membrane-bound ATPase to pump protons out and thus form a proton electrochemical gradient. The electrochemical gradient can independently be formed by the electron transport chain, during which electrons are transferred to an acceptor, usually O_2. Under these circumstances, the ATPase which is coupled to the electrochemical gradient can synthesize ATP with the energy obtained from transporting protons down the gradient.

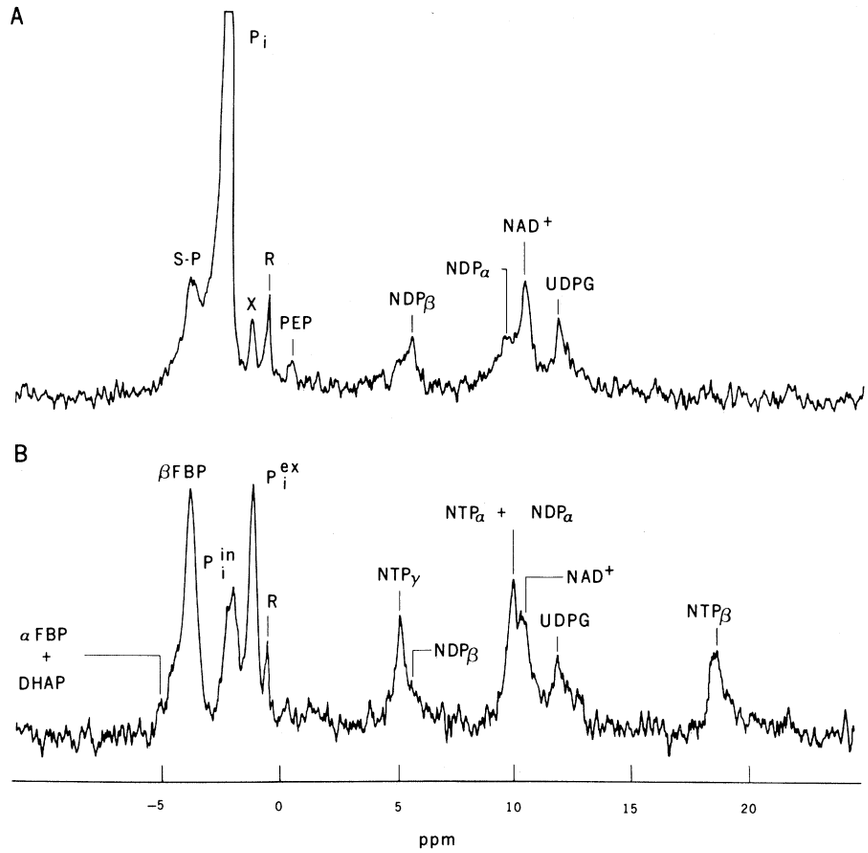

Fig. 2. Phosphorus-31 NMR spectra at 145.7 megahertz of an anaerobic *E. coli* suspension containing $\sim 5 \times 10^{11}$ cells per milliliter (A) before and (B) 4 to 6 minutes after glucose addition. Each spectrum was the sum of 400 scans with a repetition time of 0.34 second and a 45-degree radio-frequency pulse. Abbreviations: *S-P*, sugar phosphates; P_i, inorganic phosphate; P_i^{ex}, P_i^{in}, external and internal P_i, respectively; *PEP*, phosphoenolpyruvate; *NDP*, nucleoside diphosphate; *NAD*$^+$, nicotinamide adenine dinucleotide; *UDPG*, uridine diphosphate glucose; *FBP*, fructose 1,6-bisphosphate; *DHAP*, dihydroxyacetone phosphate; *NTP*, nucleoside triphosphate; and *R* is the reference signal from 0.1 percent orthophosphoric acid in 0.1*M* HCl. *X* is unassigned. [Adapted from Ugurbil *et al.* (*20*)]

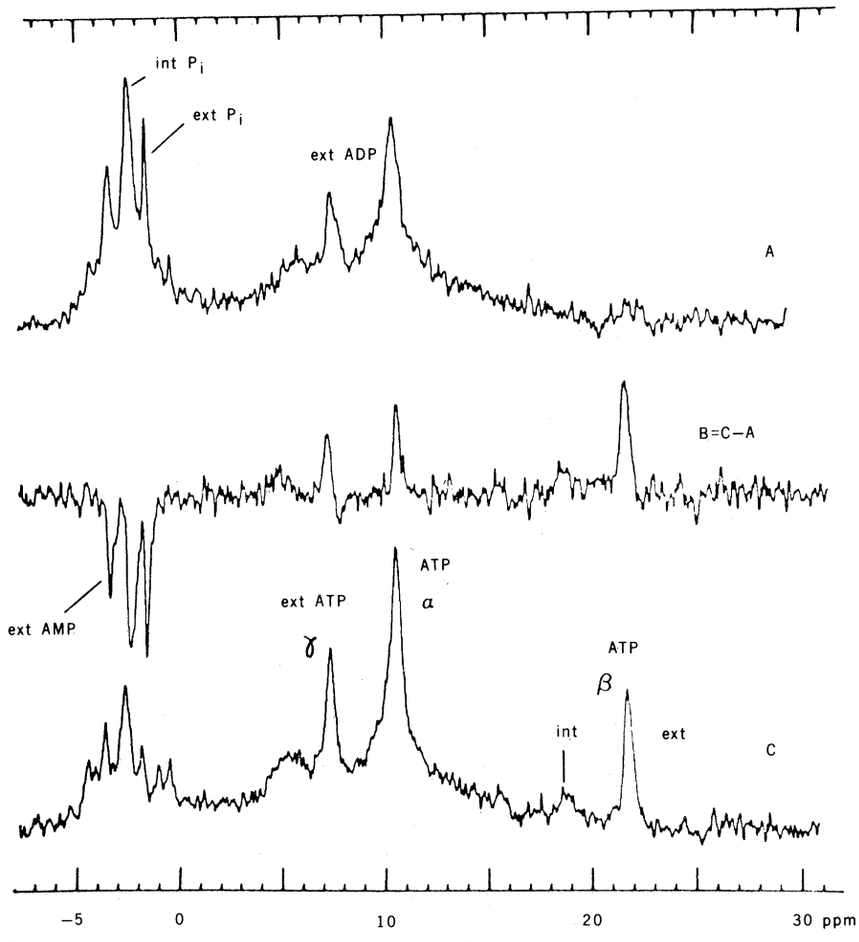

Fig. 3. Oxidative phosphorylation of external ADP by mitochondria in 0.25*M* sucrose at 0°C. (A) Ten minutes of accumulation before oxygenation. (B) The difference between (C) and (A). (C) Ten minutes of accumulation after oxygenation with 5 m*M* succinate and H_2O_2 (*25*).

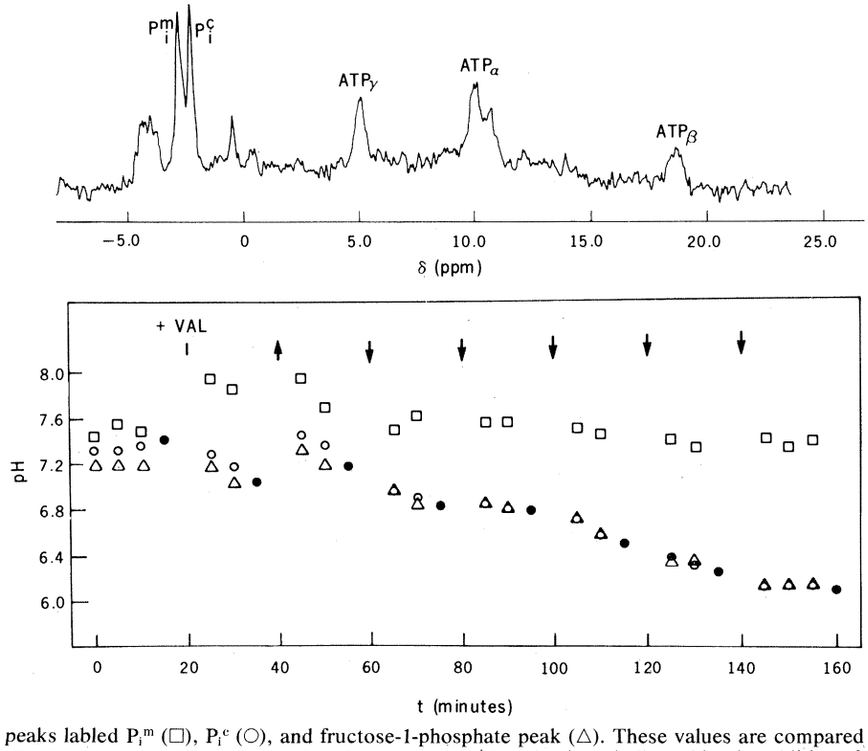

Fig. 4. The top ^{31}P NMR spectrum is a 7-minute accumulation of 1000 60°-pulses of a suspension of rat liver cells, ~20 milligrams of protein per milliliter. The sample, at 12°C, had previously been treated with valinomycin which reduced the ATP levels slightly from their normal values. The bottom shows the *p*H derived from the ^{31}P chemical shifts of the peaks labled P_i^m (□), P_i^c (○), and fructose-1-phosphate peak (△). These values are compared with the *p*H measured by an external *p*H meter (●). The external *p*H was jumped up (↑) or down (↓) at the times indicated by the addition of suitable buffers after the valinomycin (*VAL*) was added (*32*).

bic conditions (*25*). The identifications of resonances were made as in the case of *E. coli*. Similar to energized *E. coli*, mitochondria in suspension exhibit two P_i resonances, internal and external; in addition, one can detect resolved NMR peaks from external and internal pools of ADP and ATP. The latter peaks are resolved because chemical shifts of ADP and ATP depend on the degree of complexation with divalent metal ions as well as on the *p*H. From their measured chemical shifts (Fig. 3) internal ATP and ADP are shown to be predominantly bound to divalent metal ions, whereas in the suspension medium which is essentially free of divalent cations, they are uncomplexed. The NMR spectra (Fig. 3) show that, as expected, ATP is synthesized from ADP and P_i in the presence of O_2 and succinate.

Furthermore, the spectra allow us to distinguish between the internal and external pools of P_i, ADP, and ATP. Most of the ATP formed is external but some is retained inside the mitochondria. Further, the P_i consumed ultimately comes from both internal and external pools. The observed reduction in AMP occurs because of the adenylate kinase activity that catalyzes the reaction AMP + ATP → 2 ADP, which allows AMP ultimately to form ATP. In addition to showing the origin of the reactants, the difference spectra (Fig. 3B) shows clearly how oxygenation has converted external ADP primarily to external ATP and how the smaller internal pools of these energy-rich compounds have changed (*25*).

The internal ADP, ATP, and P_i concentrations have also been measured during oxygenation in the absence of externally added ADP and their concentrations used to calculate a free energy of 10 kilocalories per mole at 0°C for the internal reaction ATP ⇄ ADP + P_i. When this measurement is combined with a measure of the proton electrochemical potential and the number of protons transferred across the membrane per ATP formed, the NMR measurements will provide a quantitative test of the energetics of the chemiosmotic hypothesis.

The chemiosmotic hypothesis also

postulates that the electrochemical potential gradient is coupled to transport. Inorganic phosphate is one of the anions that is thought to distribute themselves between the intra- and extramitochondrial volumes according to ΔpH. To test this the relative distribution of P_i was measured by ^{31}P NMR in mitochondria at various values of ΔpH. The data showed unequivocally that the phosphate carrier in mitochondria acts to exchange $H_2PO_4^-$ for OH^-.

Rat Liver Cells

Although the contribution of ΔpH to the proton motive force has been previously measured in suspensions of purified mitochondria, for this to be important in vivo it is necessary that mitochondria maintain an electrochemical proton gradient with respect to the cytosol. That this in fact is the case has been demonstrated by ^{31}P NMR measurements on suspensions of rat liver cells (*22*). Figure 4 shows the ^{31}P NMR spectrum of a suspension of aerobic liver cells. The P_i peak is split into two and the upfield peak, P_i^c, corresponding to $pH = 7.10$, is assigned to the cytosol and the downfield peak, P_i^m, corresponding to $pH = 7.70$, to the mitochondria. The pH difference between cytosol and mitochondria is larger at lower external pH because the mitochondrial pH stays approximately constant in our aerobic experiments, whereas the cytosol follows the external medium. In this particular case the pH difference has been enhanced by adding valinomycin, an ionophore for K^+, which collapses $\Delta\psi$ and increases ΔpH. It has the additional effect of lowering the ATP levels, as is, in fact, observed in the liver cells (Fig. 4). Although valinomycin was used in this ^{31}P NMR experiment, a splitting could be observed in its absence, particularly when the external pH was lowered. The assignments P_i^m and P_i^c in the upper half of Fig. 4 are supported by the sequence of measurements shown in the lower half (*32*). The pH values shown were calculated from the results of another experiment on a suspension of liver cells to which fructose had been added. Under these circumstances fructose-1-phosphate (F1P) accumulates only in the cytosol. Since the F1P chemical shift is pH sensitive, its resonance provides a specific measure of the cytosolic pH. After 20 minutes, valinomycin was added and at intervals (indicated by the arrows) the external pH was "jumped" up or down with small amounts of appropriate buffers. The P_i peak labeled P_i^c gives a pH identical to that of F1P, which supports its assignment to cytosolic phosphate. Further, both P_i^c and F1P give pH values that agree with the external pH measured with a pH meter. The other inorganic phosphate peak P_i^m indicates an approximately constant pH 7.5 even when the cytosol pH has dropped as low as 6.1, and this peak is assigned to the mitochondrial phosphate.

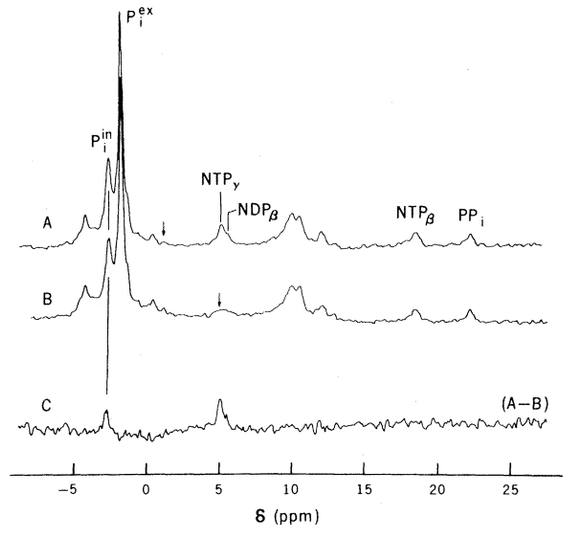

Fig. 5. Phosphate-31 NMR spectra of *E. coli* grown aerobically in glucose at 25°C in (A) the absence of and (B) during saturation of NTP_γ resonance. The samples contained about 5×10^{11} cells per milliliter. The arrows indicate the frequencies of the low-power field used. The repetition time was 0.17 second and the pulse angle was 60°. The spectra consist of 4000 scans each, taken in alternate 30-second intervals. The peaks labeled P_i^{in} and P_i^{ex} correspond to intracellular and extracellular P_i, respectively. The peak labeled PP_i at 22 ppm is polyphosphate. The peak identified as NTP_γ consists of approximately 50 percent ATP and 50 percent non-adenine triphosphates (*18*).

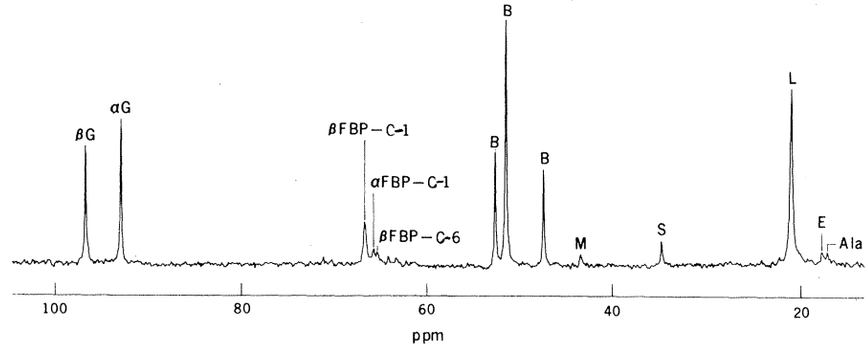

Fig. 6. A 1-minute accumulation of the ^{13}C NMR spectrum measured at 90.5 megahertz of an *E. coli* suspension at 20°C. The βG and αG are from the labeled carbon of the 50 m*M* [1-^{13}C]glucose used as substrate. The peaks labeled *B* are from the buffer, *M* is malate, *S* is from the C-2 carbon of succinate, *L* is lactate C-3, *E* is the methyl carbon of ethanol, *Ala* is alanine C-3. The FBP peaks can be seen clearly in this spectrum taken between 5 and 6 minutes after glucose addition. [Adapted from Ugurbil *et al.* (*21*)]

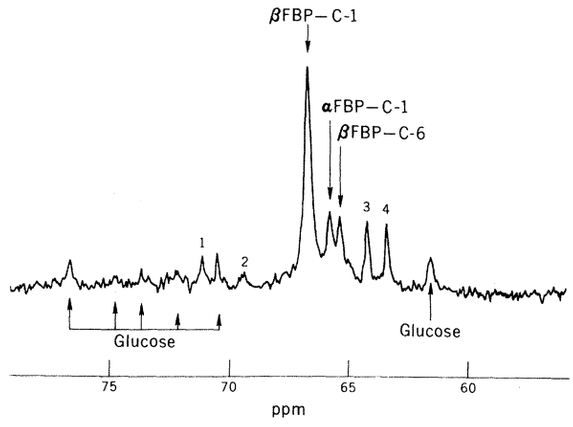

Fig. 7. The FBP region of the ^{13}C NMR spectrum of *E. coli* cells, in the presence of [1-^{13}C]glucose. The spectrum is the sum of six consecutive 1-minute spectra. The β and α anomers of FBP-C-1 are clearly seen as is the small amount of βFBP-C-6. These assignments have been checked by measuring during enzymatic digestion the NMR spectra of an extract from a similar experiment. First fructose bisphosphatase was added to convert FBP to F6P, then phosphoglucoseisomerase was used to change F6P to G6P. The resonances behaved exactly as expected, confirming the assignments (*21*).

These results, which are the first direct measurements of a *p*H gradient between cytosol and mitochondria in a whole cell, are strong support for the validity of Mitchell's chemiosmotic model applied to the eukaryotic cell. The width of the mitochondrial resonance allows us to calculate the root-mean-square spread in *p*H values inside the mitochondria; in this case it is less than 0.2 unit.

Kinetics in vivo

In addition to the types of information in the above examples, NMR studies can also supply kinetic data on the rates of reactions in vivo. This is because an individual spin will "remember" for approximately its spin lattice relaxation time, T_1, any perturbation away from its equilibrium state. Thus, if a spin on a molecule undergoing chemical exchange is saturated, that is, the population difference between the nuclear Zeeman levels is eliminated by the application of a radio-frequency field at its resonant frequency, it will transmit that saturation to the molecular species with which it is exchanging. By measuring the resultant reduction in magnetization at the resonant frequency of the second species, we can determine the unidirectional exchange rate provided the T_1's are known. This technique is known as saturation transfer (*33*, *34*).

Using this technique, we were able to measure the unidirectional rate for ATPase-catalyzed synthesis of ATP from ADP and P_i in *E. coli* (*18*). The spectra in Fig. 5 show our results at 25°C with aerobic *E. coli* cells which were respiring on endogenous carbon sources during the measurements. Figure 5A shows the typical spectrum obtained under these conditions where there are no changes in the intensities of the resonances for approximately 2 hours. Thus, the system is in a steady state. Figure 5B illustrates the spectrum of this sample obtained when the ATP position is irradiated, while in Fig. 5A (which is essentially a control experiment) the irradiating frequency was positioned halfway toward the P_i^{in} resonance (as indicated by the arrow). Figure 5C is the difference between the two. The spectra were obtained by switching the irradiating frequency between the two positions every 30 seconds for a total of 30 minutes. As shown in Fig. 5C, the two spectra cancel perfectly except in two places, the NTP_γ which is directly saturated and the *internal* P_i. The reduction of the P_i^{in} is 20 percent of its original value. After the same cells were incubated for 10 minutes with DCCD in order to inhibit the ATPase, no transfer to P_i^{in} was observed, thus showing that the exchange that transfers the saturation to P_i^{in} spins is dominated by the ATPase catalyzed reaction. Using a T_1 of 0.4 second for the P_i^{in}, which was measured on a similar DCCD-treated sample, we calculated an apparent unimolecular rate constant for the synthesis rate of ATP by the ATPase of ≈0.8 per second.

The unidirectional rate constant measured in this experiment describes the one-way flow across the ATPase and is different from net velocities measured, for example, by changes in the ATP pool as a function of time. The latter is determined by the difference between the two unidirectional rates in opposing directions; while the unidirectional rates could be very fast, the difference may in fact be very small. Indeed, in our experiments, if the O_2 is turned off, the NTP intensity decays with a time constant which is of the order of minutes, whereas the unidirectional rate we have determined for the ATPase is 0.8 per second. We emphasize here that in this experiment it has been possible to measure kinetics by NMR of a membrane-bound enzyme, a process that avoids the difficulties of solubilizing the enzyme and that keeps it coupled to an energized membrane. Furthermore, the saturation transfer measurement ensures that a particular rate is being measured, in contrast to the more conventional T_1 or T_2 measurements which respond to binding but are not specific.

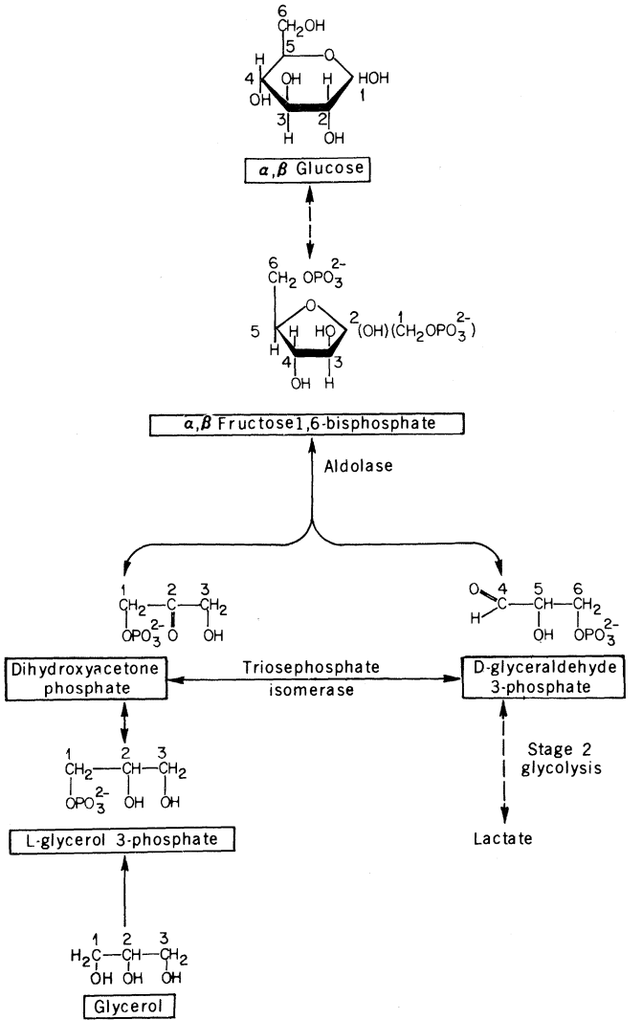

Fig. 8. Selected steps in the pathway of glucose metabolism.

Carbon-13 Nuclear Magnetic Resonance

Unlike ^{31}P, where the natural abundance is 100 percent, ^{13}C has only a 1 percent natural abundance. This has led us to use ^{13}C-enriched substrates to label various metabolic pathways, as has been done with ^{14}C. By using the techniques

we had developed to study ^{31}P NMR we have been able to follow in vivo the labeling of intermediates as well as products. In these experiments it has been possible to determine the distribution of the ^{13}C labels among the different carbons of intermediates and products. This is illustrated below by measurements of glycolysis in *E. coli* and gluconeogenesis in liver cells. In both cases, the experimental conditions were the same as those that we used in the ^{31}P studies, so that the spectra obtained as the *E. coli* catabolized glucose or the liver cells synthesized it could be correlated with the internal *p*H values and ATP levels, for example, that we had obtained using ^{31}P NMR.

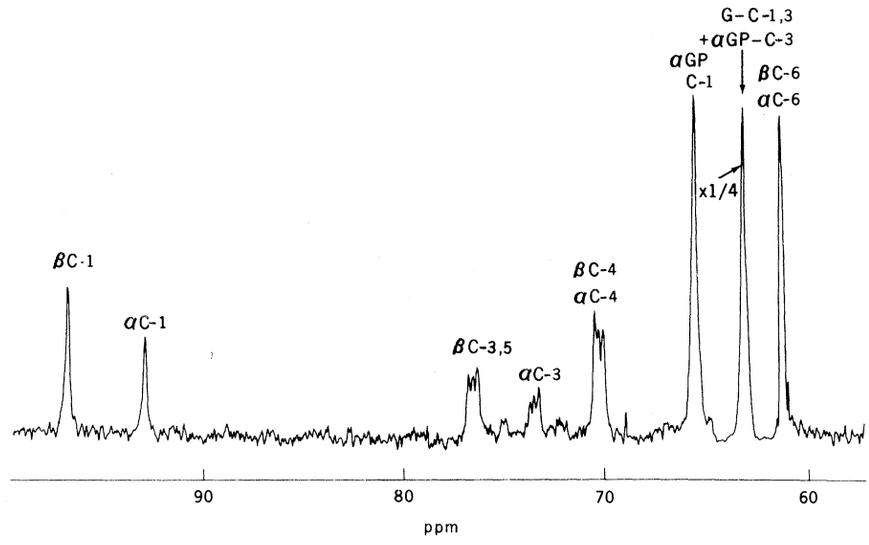

Fig. 9. Carbon-13 NMR spectrum at 25°C of rat liver cells from a normal rat, accumulated between 18 and 35 minutes after the introduction of 22 m*M* [1,3-^{13}C] glycerol. Glucose is labeled strongly at the 1, 3, 4, and 6 carbon positions of the α and β anomers of glucose. Note that the carbon-carbon spin coupling has split the lines from C-3 and C-4 of glucose. G-C-1,3 is the labeled glycerol peak, and αGP is L-glycerol 3-phosphate. [Adapted from Cohen *et al.* (*24*)]

Escherichia coli

An example of the spectra obtainable (*21*) by feeding enriched glucose to *E. coli* is shown in Fig. 6. The spectrum is a 1-minute accumulation taken between 5 and 6 minutes after [1-^{13}C]glucose was added to the anaerobic *E. coli* suspension. The specific assignments, given in the figure, were made as before on the basis of chemical shifts, behavior in extracts, and, in one case discussed below, by enzymatic digestion of the compound. When glucose was first added to the sample, the NMR spectrum reflected that the glucose was in anomeric equilibrium with a 64 : 36 ratio of β : α anomers. The lower concentration of the β form, seen 6.5 minutes after glucose addition (Fig. 6), indicates that this particular strain of *E. coli*, MRE 600, preferentially catabolizes the α-anomer; this preference was not observable in three other *E. coli* strains because, unlike MRE 600, they displayed rapid anomerase activity. *Escherichia coli* cells are capable of producing varying ratios of glycolytic products depending on their environment. In Fig. 6 the dominant product is lactate, but succinate, malate, ethanol, and acetate are also present in small quantities, the last not being observed in the particular spectrum shown. In addition to the end products in Fig. 6, it is possible to observe fuctose bisphosphate (FBP), the major intermediate of glycolysis in *E. coli*. The internal concentration of this metabolite was estimated to be ~13 m*M* from the ^{31}P studies. The time sequences of the ^{13}C and ^{31}P NMR spectra indicate that FBP increases in 1 or 2 minutes to a constant value that is maintained until the concentration of glucose drops to less than 10 percent of its initial value. Afterward, the FBP drops to zero in 4 minutes, remaining visible for 2 minutes after the glucose has completely vanished.

The FBP region of the spectrum is expanded in Fig. 7, where six 1-minute consecutive spectra, which displayed constant FBP intensity, were added together to improve the signal-to-noise ratio. Note that the peak at 65.8 ppm has been assigned to the C-1 of αFBP. From the relative intensities of the peaks of the α- and βFBP we have concluded that FBP is an anomeric equilibrium, in vivo. This measurement shows one of the advantages of obtaining NMR measurements in vivo: the time for FBP anomerization is about 1 second, so that it would be very difficult to avoid some equilibration while extracting the FBP.

In addition to the time course that can be obtained from sequential spectra taken at 1-minute intervals, more detailed rate information can be obtained from the observation of a label at the peak assigned to the C-6 of βFBP (Fig. 7). The presence of this peak shows that some of the label, introduced at C-1 of glucose and therefore expected to flow into the C-1 of FBP, has been "scrambled" to the C-6 FBP position. From this it is possible to calculate the degree of disequilibrium of different enzymatic steps, in vivo. This can be understood by reference to Fig. 8, which shows some of the reactions involved in glucose metabolism. The relevant reactions are those catalyzed by aldolase and triosephosphate isomerase (TPI). For example, if the aldolase triangle had rates that were rapid compared to the through rate and hence the constituents were at equilibrium, then the C-1 and C-6 peaks of FBP would have equal intensities. At the other extreme, if the flux were very fast compared with the reactions that mix the label, then no "scrambling" would be observed. By repeating the experiment using [6-^{13}C]glucose we have shown that no "scrambling" in the reverse direction is observed to within an accuracy of 5 percent. Although an unequivocal assignment of the pathway responsible for the "scrambling" observed requires a detailed analysis, it is evident from these results that there is considerably more flux through aldolase toward the trioses than there is in the reverse direction.

In similar experiments on yeast it has been found that, in contrast to the results with *E. coli*, the "scrambling" itself is much larger and is approximately equal in the two directions. In this case, the data seem to be fitted reasonably by the simple aldolase-TPI triangle with TPI close to equilibrium and a back flux through aldolase almost as large as the forward flux (*35*).

Rat Liver Cells

Similar kinds of information can be obtained from suspensions of liver cells performing gluconeogenesis (*24*). Figure 9 shows a ^{13}C NMR spectrum accumulated during the period 18 to 35 minutes after [1,3-^{13}C]glycerol was added to a

suspension of rat liver cells. Glycerol and α-glycerophosphate (αGP), which is an intermediate in glycerol metabolism, are detectable in the spectrum together with glucose, which is synthesized from glycerol by way of the well-established pathway outlined in Fig. 8. To a first approximation all the ^{13}C label appears in the 1, 3, 4, and 6 carbons of glucose, exactly as expected. Consecutive spectra recorded after glycerol addition (Fig. 9 was taken from one such series), allow one to follow the time course of the ^{13}C distribution in glycerol, αGP, and glucose. Differences in the rates of synthesis of these metabolites and others, such as lactate and alanine, have been measured in liver cells from normal and hyperthyroid rats. In the latter, the glycerol consumption and glucose synthesis rates were several times faster and the concentration of αGP was several times lower. From these data we determined the flux of αGP through the cytosolic and mitochondrial αGP-dehydrogenases. These results agreed with measurements obtained in vitro which had shown that the mitochondrial αGP-dehydrogenase rate is increased in the cells from the hyperthyroid rats. Several other differences between the hyperthyroid and the normal rat livers were revealed by the NMR experiments, demonstrating the usefulness of the simultaneity available from NMR spectra in understanding the complex cellular reaction to hormonal stimulation (*24*).

In Fig. 9 the peaks labeled C-3 and C-4 appear to be triplets. The triplets arise from the spin-spin coupling that occurs whenever a ^{13}C is next to another ^{13}C. Thus, if a glucose molecule was formed by condensing two 1,3-^{13}C-labeled trioses, then the resonances at positions 3 and 4 would both be split into doublets, while if only one of the trioses were labeled there would be only a single peak. Thus, by comparing the intensity of the center peak (the unpaired label) with the intensity of the wings (the paired label) it is possible to calculate the amount of unlabeled substrate incorporated into the glucose. This enables one to interpret a single NMR spectrum in terms of the amount of label incorporated in the glucose, as well as in terms of the total glucose produced.

Another important point is the equality of label in the two halves of the glucose molecule (that is, carbons 1, 2, 3 and 4, 5, 6). In all experiments with glycerol, even when unlabeled substrate enters the synthesis path, the two halves of the resulting glucose are equally labeled. This requires either that the TPI reaction be in equilibrium or that other fluxes through the triose pool be negligible.

The existence of any flux through the pentose cycle can be determined quantitatively from the observed label distribution. For example, it has been observed that [2-^{13}C]glycerol produces glucose with 10 percent of its label moved from the C-2 to the C-1 position (but not from the C-5 to the C-6) (*24*). From this it was possible to calculate that about 10 percent of the hexoses have been cycled through the pentose pathway and to estimate the relative fluxes through the transketolase and transaldolase subpaths.

Conclusions

We have reviewed recent experiments on *E. coli*, rat liver cells, and purified rat liver mitochondria with the aim of demonstrating the quality of information that can be obtained from experiments with ^{31}P and ^{13}C NMR. From the former one obtains simultaneously the internal *p*H and considerable information about the distribution and concentrations of phosphorylated metabolites. It has been possible to observe, we believe for the first time, a *p*H difference between cytosol and mitochondria in an intact cell. These, together with the results on P_i transport and ATP formation in isolated mitochondria, support Mitchell's chemiosmotic model. In addition, it has been possible, by using saturation transfer, to measure a true unidirectional rate in vivo, namely, the ATPase synthesis rate in aerobic *E. coli*. From ^{13}C NMR further information on in vivo rates can be obtained by observing the amount of "scrambling" in a particular metabolic pathway. For example in *E. coli*, one can conclude that during glycolysis the aldolase is out of equilibrium. It is clear that ^{31}P and ^{13}C NMR measurements allow one to follow the details of metabolism and bioenergetics in vivo.

References and Notes

1. R. B. Moon and J. H. Richards, *J. Biol. Chem.* **248**, 7276 (1973).
2. T. O. Henderson, A. J. R. Costello, A. Omachi, *Proc. Natl. Acad. Sci. U.S.A.* **71**, 2487 (1974).
3. R. K. Gupta, J. L. Benovic, Z. B. Rose, *J. Biol. Chem.* **253**, 6172 (1978).
4. J. M. Salhany, T. Yamane, R. G. Shulman, S. Ogawa, *Proc. Natl. Acad. Sci. U.S.A.* **72**, 4966 (1975).
5. G. Navon, S. Ogawa, R. G. Shulman, T. Yamane, *ibid.* **74**, 87 (1977).
6. D. I. Hoult, S. J. W. Busby, D. G. Gadian, G. K. Radda, R. E. Richards, P. J. Seeley, *Nature (London)* **252**, 285 (1974).
7. C. T. Burt, T. Glonek, M. Barany, *J. Biol. Chem.* **251**, 2584 (1976).
8. D. P. Hollis, R. L. Nunnally, W. E. Jacobus, G. J. Taylor, *Biochem. Biophys. Res. Commun.* **75**, 1086 (1977).
9. P. B. Garlick, G. K. Radda, P. J. Seeley, B. Chance, C. Barlow, *Proc. Natl. Acad. Sci. U.S.A.* **73**, 4446 (1976).
10. P. A. Sehr, G. K. Radda, P. J. Bore, R. A. Sells, *Biochem. Biophys. Res. Commun.* **77**, 195 (1977).
11. G. Navon, R. Navon, R. G. Shulman, T. Yamane, *Proc. Natl. Acad. Sci. U.S.A.* **75**, 891 (1978).
12. F. E. Evans and N. O. Kaplan, *ibid.* **74**, 4909 (1977).
13. K. Ugurbil, R. G. Shulman, H. Holmsen, J. Costa, *Biophys. J.* **21**, 147A (1978).
14. R. G. Johnson, A. Scarpa, L. Salganicoff, *Frontiers of Biological Energetics*, P. L. Dutton, J. Leigh, A. Scarpa, Eds. (Academic Press, New York, 1978).
15. R. D. Casey, D. Njus, G. K. Radda, P. A. Sehr, *Biochemistry* **16**, 972 (1977).
16. C. T. Burt, S. M. Cohen, M. Barany, *Annu. Rev. Biophys. Bioeng.* **8**, 1 (1979).
17. G. Navon, S. Ogawa, R. G. Shulman, T. Yamane, *Proc. Natl. Acad. Sci. U.S.A.* **74**, 888 (1977).
18. T. R. Brown, K. Ugurbil, R. G. Shulman, *ibid.*, p. 5551.
19. S. Ogawa, R. G. Shulman, P. Glynn, T. Yamane, G. Navon, *Biochim. Biophys. Acta* **502**, 45 (1978).
20. K. Ugurbil, H. Rottenberg, P. Glynn, R. G. Shulman, *Proc. Natl. Acad. Sci. U.S.A.* **75**, 2244 (1978).
21. K. Ugurbil, T. R. Brown, J. A. den Hollander, P. Glynn, R. G. Shulman, *ibid.*, p. 3742.
22. S. M. Cohen, S. Ogawa, H. Rottenberg, P. Glynn, T. Yamane, T. R. Brown, R. G. Shulman, *Nature (London)* **273**, 554 (1978).
23. S. M. Cohen, S. Ogawa, R. G. Shulman, in *Frontiers of Biological Energetics*, P. L. Dutton, J. Leigh, A. Scarpa, Eds. (Academic Press, New York, 1978), p. 1357.
24. S. M. Cohen, S. Ogawa, R. G. Shulman, *Proc. Natl. Acad. Sci. U.S.A.* **76**, 1603 (1979).
25. S. Ogawa, H. Rottenberg, T. R. Brown, R. G. Shulman, C. L. Castillo, P. Glynn, *ibid.* **75**, 1796 (1978).
26. R. T. Eakin, L. O. Morgan, C. T. Gregg, N. A. Matwiyoff, *FEBS Lett.* **28**, 259 (1972).
27. U. Séquin and A. I. Scott, *Science* **186**, 101 (1974).
28. M. Kainosho, K. Ajisaka, H. Nakazawa, *FEBS Lett.* **80**, 385 (1977).
29. P. Mitchell, *Nature (London)* **191**, 144 (1961).
30. F. M. Harold, *Curr. Top. Bioenerg.* **6**, 89 (1977).
31. P. D. Boyer, B. Chance, L. Ernster, P. Mitchell, E. Racker E. C. Slater, *Annu. Rev. Biochem.* **46**, 966 (1977).
32. S. M. Cohen, S. Ogawa, R. G. Shulman, in preparation.
33. S. Forsen and R. A. Hoffman, *J. Chem. Phys.* **26**, 958 (1963).
34. R. K. Gupta and A. G. Redfield, *Science* **169**, 1204 (1970).
35. J. A. den Hollander, T. R. Brown, K. Ugurbil, R. G. Shulman, in preparation.

36. S.M.C. was supported in part by a fellowship from the American Cancer Society, and J.A.d.H. in part by a fellowship from the Netherlands Organization for the Advancement of Pure Research (Z.W.O.).